

Chapter 2. Creating a Spatially Heterogeneous Scalar Quantity

Our objective is to create spatially heterogeneous stress that has appropriate spectral properties for the real Earth. In this chapter, we will address how to produce one scalar component of heterogeneous stress, and in the next chapter, we will show how we construct the complete 3D deviatoric stress tensor with five independent components.

Liu-Zeng et al. [2005] estimated slip heterogeneity in the real Earth by comparing slip vs. length scaling in the real Earth to the scaling predicted by different mathematical models of slip heterogeneity. Their equation for generating heterogeneous slip is

$$D(x) = D_0 |R(x) * F(x)| = D_0 \left| FT^{-1} \left[\hat{R}(k) k^{-\gamma} \right] \right| \quad (2.1)$$

where $D(x)$ is slip as a function of position, $R(x)$ is a Gaussian random function of x with zero mean and variance of 1.0, $F(x)$ is a spatial filter, $\hat{R}(k)$ is the Fourier transform of $R(x)$, and $k^{-\gamma}$ is the Fourier transform of $F(x)$ where k is the spatial wavenumber, and γ is a constant [Liu-Zeng, et al., 2005]. We use γ as the filtering symbol for Liu-Zeng et al. instead of α , to distinguish between the slip filtering in their paper vs. the stress filtering in this thesis. They find that $1.25 < \gamma < 1.5$ best describes slip vs. length data in the real Earth.

In our studies, we are interested primarily in stress, which along faults should have the same spectrum as the spatial derivatives of slip. In particular, Hooke's law connects stress and strain

$$\sigma_{ij} = \lambda(\epsilon_{kk})\delta_{ij} + 2\mu\epsilon_{ij} \quad (2.2)$$

where $i = 1, 2, 3$ and $j = 1, 2, 3$, and λ and μ are constants known as Lamé parameters.

Strain, $\varepsilon_{ij} = \frac{1}{2} \left(\frac{\partial u_i}{\partial x_j} + \frac{\partial u_j}{\partial x_i} \right)$, where $\frac{\partial u_i}{\partial x_j}$ is the derivative of the i th component of

displacement in the j th direction. Therefore, stress along faults should have spatial roughness equivalent to the spatial derivative of slip.

If the displacement along a 1D cross section can be described as

$$D(x) = D_0 \left| FT^{-1} \left[\hat{R}(k_x) k_x^{-\gamma} \right] \right|, \quad (2.3)$$

then a single scalar component of the stress tensor along a 1D cross section can be filtered as follows:

$$\begin{aligned} \sigma_{xx}(x) &\propto \frac{dD(x)}{dx} = D_0 \left| FT^{-1} \left[\hat{R}(k_x) k_x k_x^{-\gamma} \right] \right| \\ &= D_0 \left| FT^{-1} \left[\hat{R}(k_x) k_x^{(1-\gamma)} \right] \right| = D_0 \left| FT^{-1} \left[\hat{R}(k_x) k_x^{-\alpha} \right] \right| \end{aligned} \quad (2.4)$$

where $\alpha = \gamma - 1$. Consequently, if we wish to have appropriate length vs. slip scaling in the real Earth, we should have heterogeneous stress with $0.25 < \alpha < 0.5$ along 1D cross sections.

For our purposes we produce a suite of different heterogeneous stresses ranging from $\alpha = 0.0$ to $\alpha = 1.5$ and compare these to real Earth data in Chapter 5 to find an optimal α . Note that $\alpha = 1.0$ produces spatially filtered stress that has smoothing equivalent to integrating Gaussian white noise once. An $\alpha = 0.5$ produces spatially filtered stress that has smoothing equivalent to fractionally integrating Gaussian white noise, 0.5 times, etc. Figures 2.1 and 2.2 demonstrate how this filter operates for filtered Gaussian white noise.

Figures 2.3 and 2.4 show spatially filtered Gaussian white noise for $\alpha = 0.0$ (our test case, which should have a flat spectral slope for no filtering) and $\alpha = 0.5$ (filtered white noise that yields smoothness equivalent to a fractional integration of 0.5).

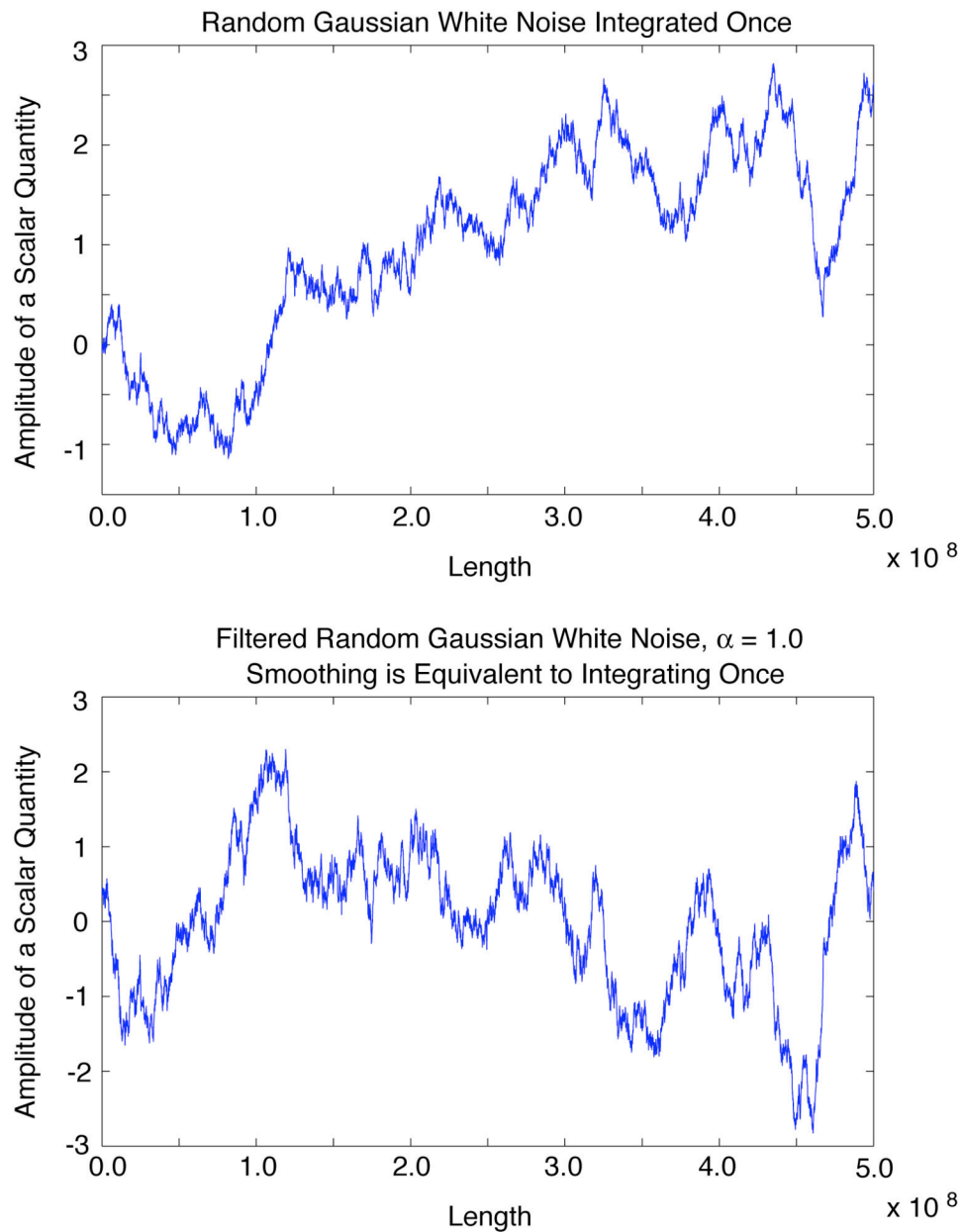


Figure 2.1. *Gaussian white noise is integrated once (top panel) and is filtered with $\alpha = 1.0$ (bottom panel). While the functions look different since one is an integral and the other is simply smoothing the Gaussian noise, they have approximately the same degree of spatial heterogeneity.*

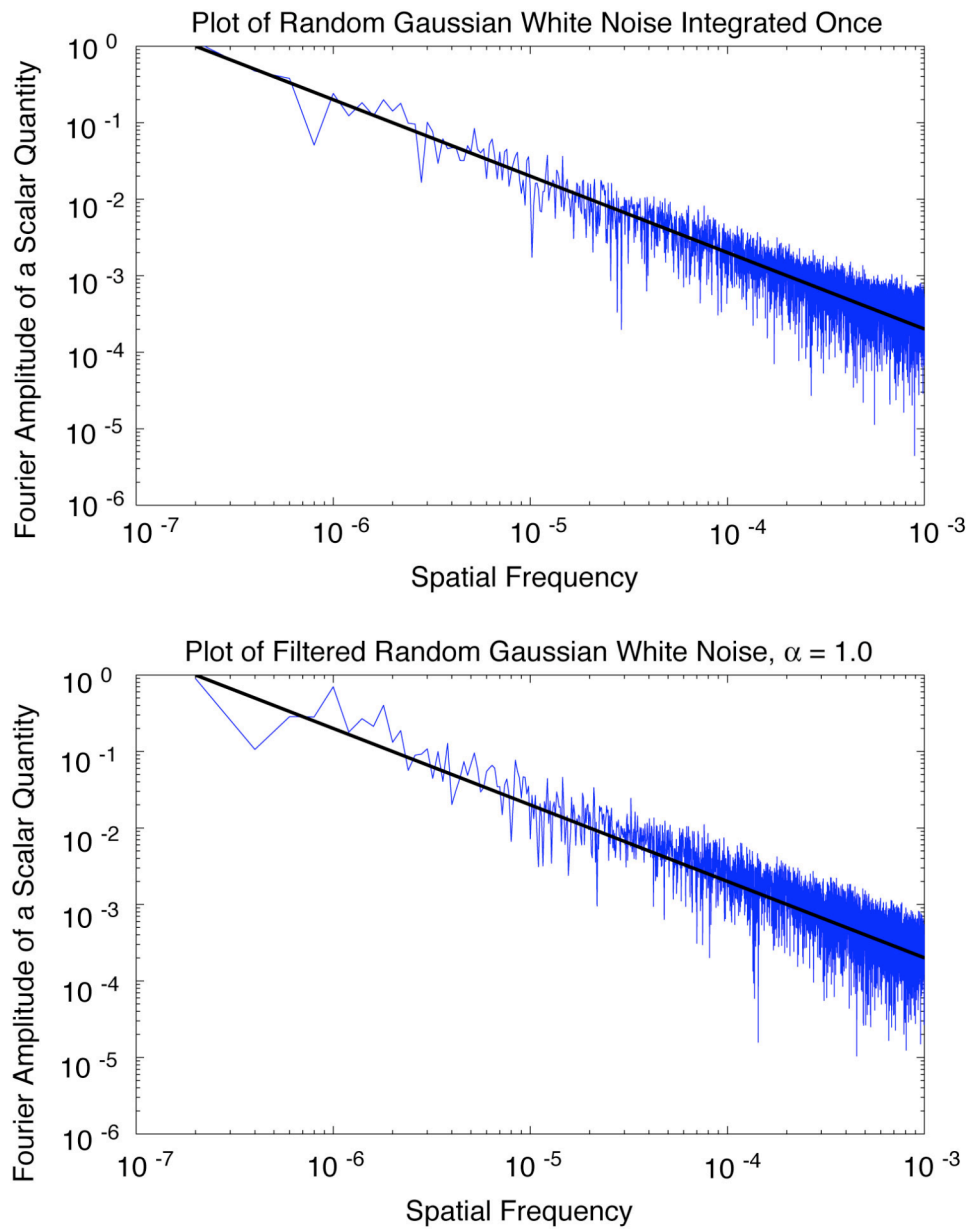


Figure 2.2. The Fourier spectral amplitude is plotted for the integrated Gaussian white noise (top panel) and filtered Gaussian white noise with $\alpha = 1.0$ (bottom panel). A black line with slope = -1 is plotted on both the top and bottom panels.

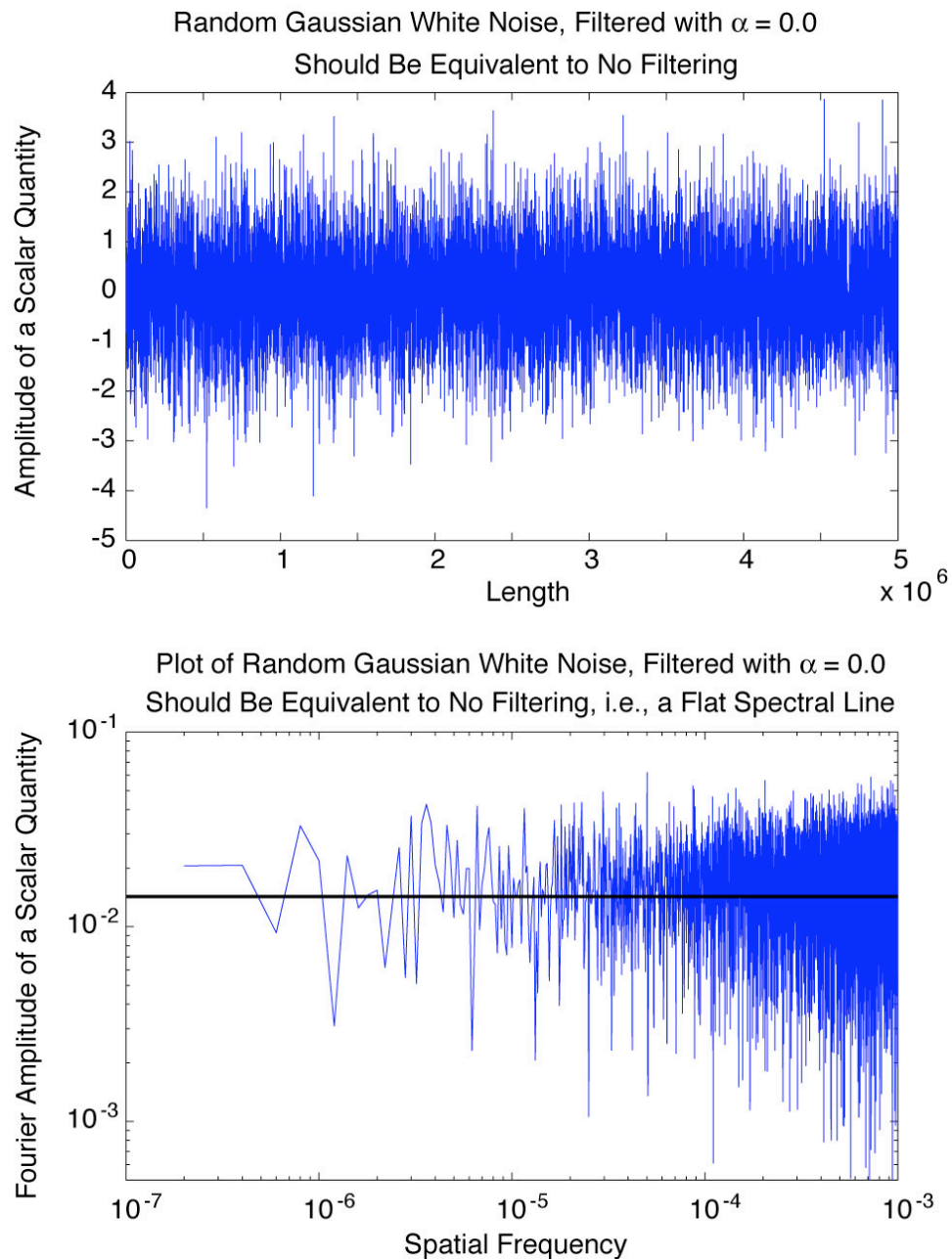


Figure 2.3. *Gaussian white noise in the top panel. Filtering with our smoothing parameter, $\alpha = 0.0$, which is equivalent to no smoothing. The bottom panel is a log-log plot of the Fourier amplitude spectra of the noise vs. spatial frequency. Since $\alpha = 0.0$, the slope of the Fourier amplitude spectra for the log-log plot = 0, as expected. This figure simply shows our baseline test case.*

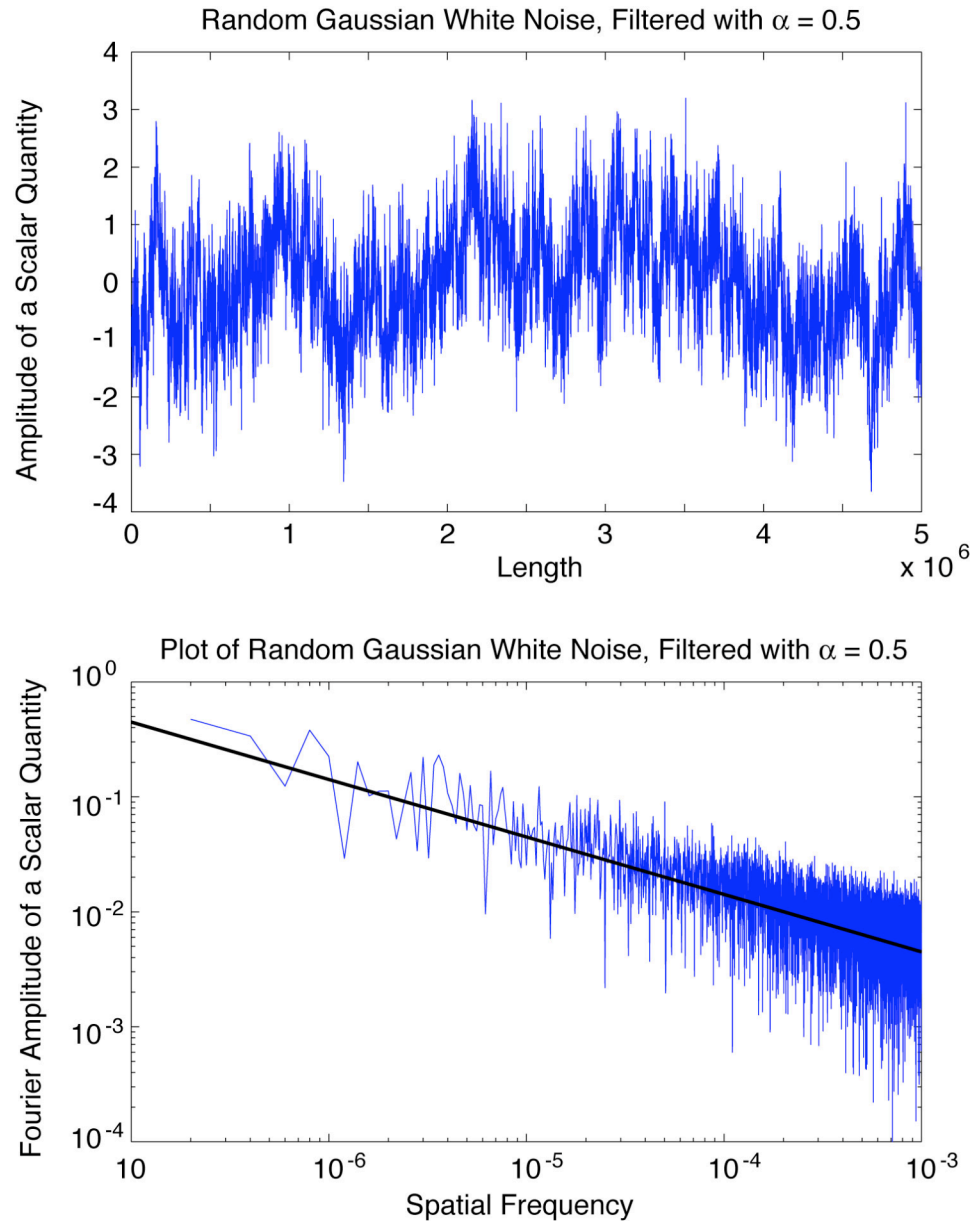


Figure 2.4. *In this case, our Gaussian white noise is filtered with an $\alpha = 0.5$ in the top panel. The bottom panel is the log-log plot of the Fourier amplitude spectrum of our filtered noise vs. spatial frequency. Note that the slope of the trend ≈ -0.5 . This is the approximate desired slope for a filtering parameter of $\alpha = 0.5$.*

So far all the results presented have been for 1D Gaussian white noise. Now we need to extrapolate the results to 2D and 3D, since our simulations will require a 3D grid of spatially smoothed Gaussian white noise to represent the spatially heterogeneous stress. One constraint we place on this extrapolation is that any 1D cross section through a 2D or 3D grid should have the same spectral falloff as our simple 1D examples. A common equation that is used for filtering random Gaussian white noise in multiple dimensions is the Spectral Approximation [Barnsely, *et al.*, 1988],

$$F(k_1, k_2, \dots, k_n) \propto \frac{1}{\left(\sqrt{\sum_{i=1}^n k_i^2} \right)^{\frac{2H+n}{2}}} \quad (2.5)$$

where $F(k_1, k_2, \dots, k_n)$ is the n -dimensional filter we convolve with our noise, and H is the Hurst exponent. H relates to α as follows: $\alpha = \frac{2H+1}{2}$, where α describes the spectral falloff of any 1D straight line within our multidimensional grid. So we can rewrite this filter as

$$F(k_1, k_2, \dots, k_n) \propto \frac{1}{\left(\sqrt{\sum_{i=1}^n k_i^2} \right)^{A(\alpha, n)}} \quad (2.6)$$

where

$$A(\alpha, n) = \alpha + \frac{(n-1)}{2}. \quad (2.7)$$

The filter exponent, $A(\alpha, n)$, in 1D simplifies to

$$A_{1D}(\alpha) = \alpha, \quad (2.8)$$

which means, $F(k_1) = \frac{1}{k_1^\alpha}$, the 1D falloff we want.

However for 2D and 3D, we find that the approximation is more limited. For 2D we have

$$A_{2D}(\alpha) = (\alpha + 0.5), \quad (2.9)$$

and in 3D

$$A_{3D}(\alpha) = (\alpha + 1). \quad (2.10)$$

These equations are typically used for the range, $0.5 < \alpha < 1.5$. As α approaches 0 (no filtering, just random Gaussian white noise), the Spectral Approximation breaks down, because we have

$$\begin{aligned} A_{2D}(0) &= 0.5 \neq 0 \\ A_{3D}(0) &= 1.0 \neq 0 \end{aligned}$$

while we need $A(\alpha, n) \rightarrow 0$ as $\alpha \rightarrow 0$ to generate Gaussian white noise.

For example, in 2D we would have

$$F(k_1, k_2) \propto \frac{1}{\left(\sqrt{\sum_{i=1}^2 k_i^2} \right)^{1/2}},$$

which produces filtered, fractal noise, instead of what we want,

$$F(k_1, k_2) \propto \frac{1}{\left(\sqrt{\sum_{i=1}^2 k_i^2} \right)^0} = 1,$$

which maintains the Gaussian random noise. We will be testing a range of $0.0 < \alpha < 1.5$, which has values of α that fall out of the commonly accepted range of $0.5 < \alpha < 1.5$; therefore, we need to develop a better approximation.

To visually display this need for a better approximation, we filter 2D and 3D grids with many different exponents for the filtering transfer function, $F(k_1, k_2, \dots, k_n)$, plot their respective 1D spectral falloffs, and then plot $A(\alpha, n)$ vs. α . In essence, we are numerically computing the actual relationship between the exponent function, $f(\alpha, n)$,

and α , where $F(k_1, k_2) \propto \frac{1}{\left(\sqrt{\sum_{i=1}^2 k_i^2}\right)^{f(\alpha, n)}}$. Then we are comparing this numerically

computed value to the spectral approximation, $A(\alpha, n)$, to demonstrate any discrepancies. Figure 2.5 shows the 2D and 3D results of this numerical test.

To address the problems with $A(\alpha, n)$ as $\alpha \rightarrow 0$, we develop a new approximation to $f(\alpha, n)$, the actual exponent function. Note that this new approximation is geared toward our particular size of grids, 201x201x201 points. When the number of points, N , along any one dimension is sufficiently large, the filtering exponent becomes stable, but for grids with $N = 201$, there is an added effect due to the finite size of the grid. Hence, our new approximation is only valid for this size of grid. For our new approximation we define:

$$F(k_1, k_2, \dots, k_n) \propto \frac{1}{\left(\sqrt{\sum_{i=1}^n k_i^2}\right)^{B(\alpha, n)}} \quad (2.11)$$

where $B(\alpha, n)$ is our new exponent function. For 2D

$$B_{2D}(\alpha) = 2\sqrt{\left[\left(\frac{\alpha + 2.5}{2.25}\right)^2 - 1\right]} - 1, \quad (2.12)$$

and for 3D

$$B_{3D}(\alpha) = 4.5 \sqrt{\left[\left(\frac{\alpha + 7.5}{7.45} \right)^2 - 1 \right]} - 0.5. \quad (2.13)$$

Figure 2.6 compares these new approximations to our numerically determined, $f(\alpha, n)$, exponent function. Note, by design they are so closely matched it is difficult to distinguish one from another. $B(\alpha, n)$ plots almost on top of $f(\alpha, n)$ for both 2D ($n = 2$) and 3D ($n = 3$).

Now that we have a new approximation that produces the appropriate spectral properties for 2D and 3D data sets, we display some results in Figures 2.7 and 2.8, using $\alpha = 0.0, 0.5, \text{ and } 1.0$. We find that as α increases the scalar quantity becomes increasingly smooth spatially, i.e., the scalar values have increasing spatial correlation. Using the new approximation, the results for 2D and 3D have similar properties, with 1D spectral falloffs described by α .

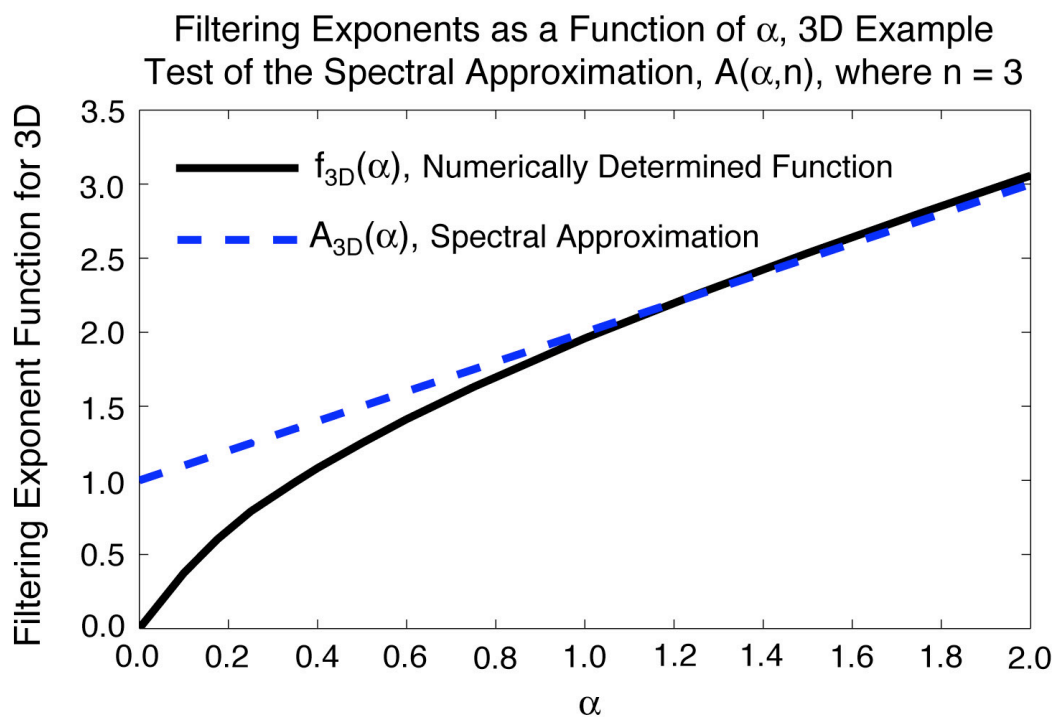
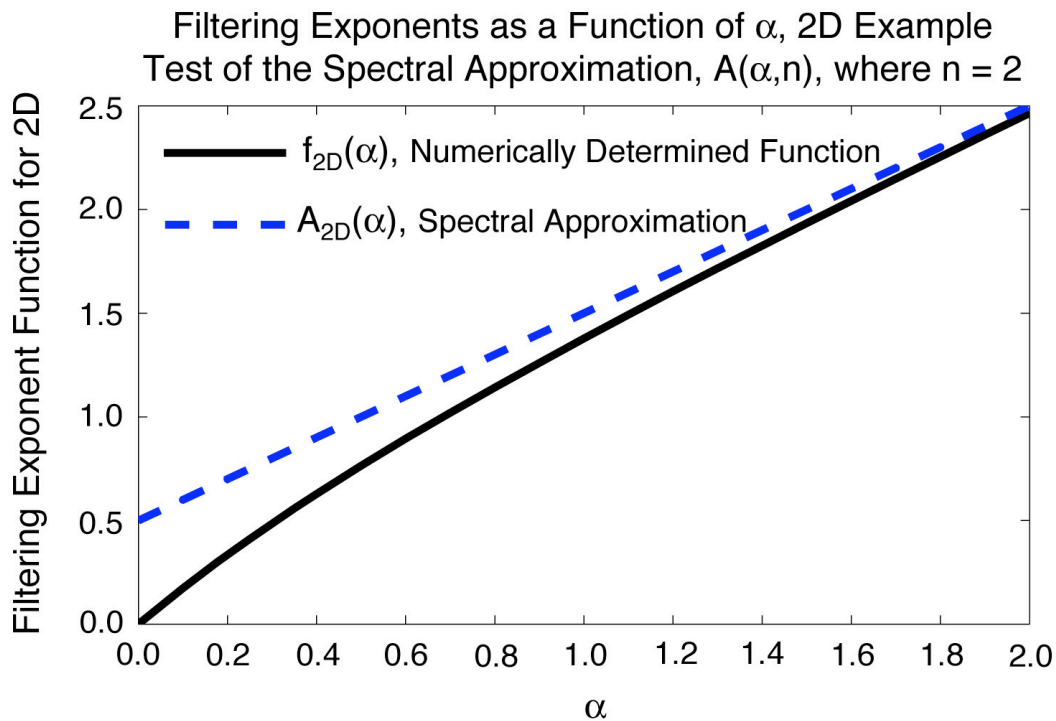


Figure 2.5. When we filter scalar values in 2D and 3D, we still desire that any 1D cross section maintain the $-\alpha$ slope. For 1D grids, we could simply use the fractal filter,

$F(k_1) = \frac{1}{k_1^\alpha}$, to produce a $-\alpha$ slope, but in 2D and 3D it becomes more complicated.

For multiple spatial dimensions, the exponent on the filter can now be expressed as a function of α , i.e., as a function of the desired 1D cross-sectional smoothness. This figure shows the following in 2D (top panel) and 3D (bottom panel). The solid black line is a plot of $f(\alpha, n)$ vs. α , determined from numerical simulations for a 201x201x201

grid, where $F_f(k_1, k_2, \dots, k_n) \propto \frac{1}{\left(\sqrt{\sum_{i=1}^n k_i^2}\right)^{f(\alpha, n)}}$, and α describes the 1D spectral falloff of

Gaussian white noise filtered with $F_f(k_1, k_2, \dots, k_n)$. The dashed blue line is a plot of

$A(\alpha, n)$ vs. α where $A(\alpha, n)$ is the Spectral Approximation function used in the filter,

$F_A(k_1, k_2, \dots, k_n) \propto \frac{1}{\left(\sqrt{\sum_{i=1}^n k_i^2}\right)^{A(\alpha, n)}}$. $A(\alpha, n) = \alpha + \frac{(n-1)}{2}$ [Barnsely, et al., 1988] where

n is the number of spatial dimensions and α is the 1D spectral falloff of Gaussian white noise filtered with $F_A(k_1, k_2, \dots, k_n)$. We wish to find a function that accurately describes

the numerically determined curve, $f(\alpha, n)$; hence, if $A(\alpha, n)$ is a good approximation, it

will plot directly on top of $f(\alpha, n)$. Unfortunately, this figure shows that the Spectral

Approximation, designated by $A(\alpha, n)$ becomes a poor approximation for small values of

α . Most of our simulations use a range of $0.0 \leq \alpha \leq 1.0$, where this approximation has

trouble; hence, a better approximation for 2D ($n = 2$) and 3D ($n = 3$) is needed.

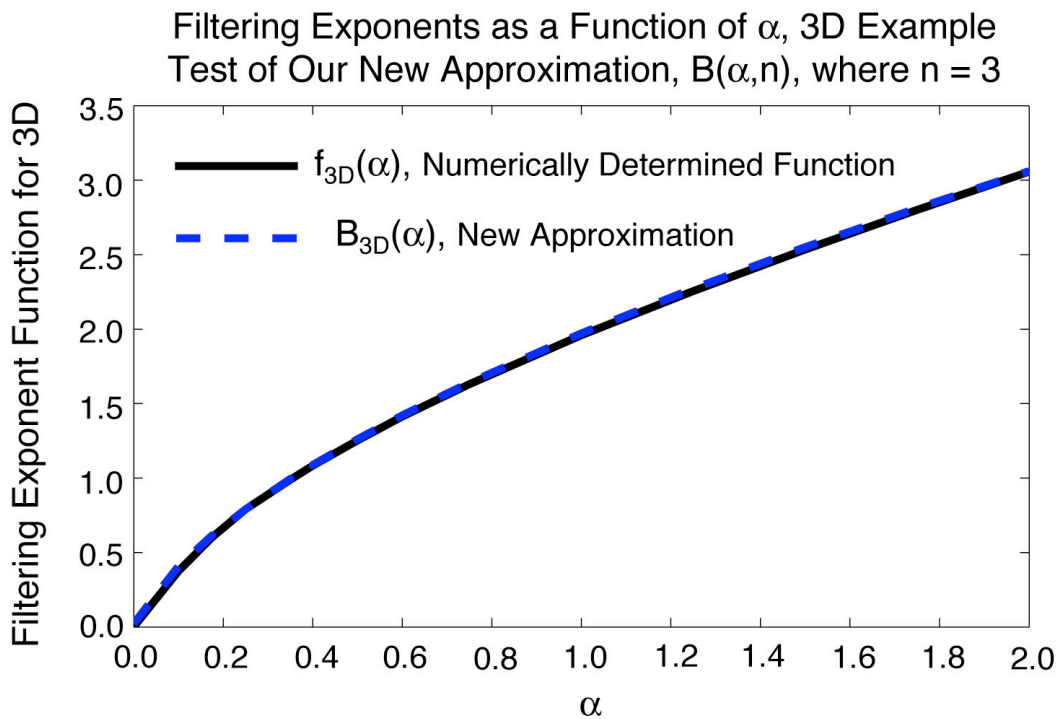
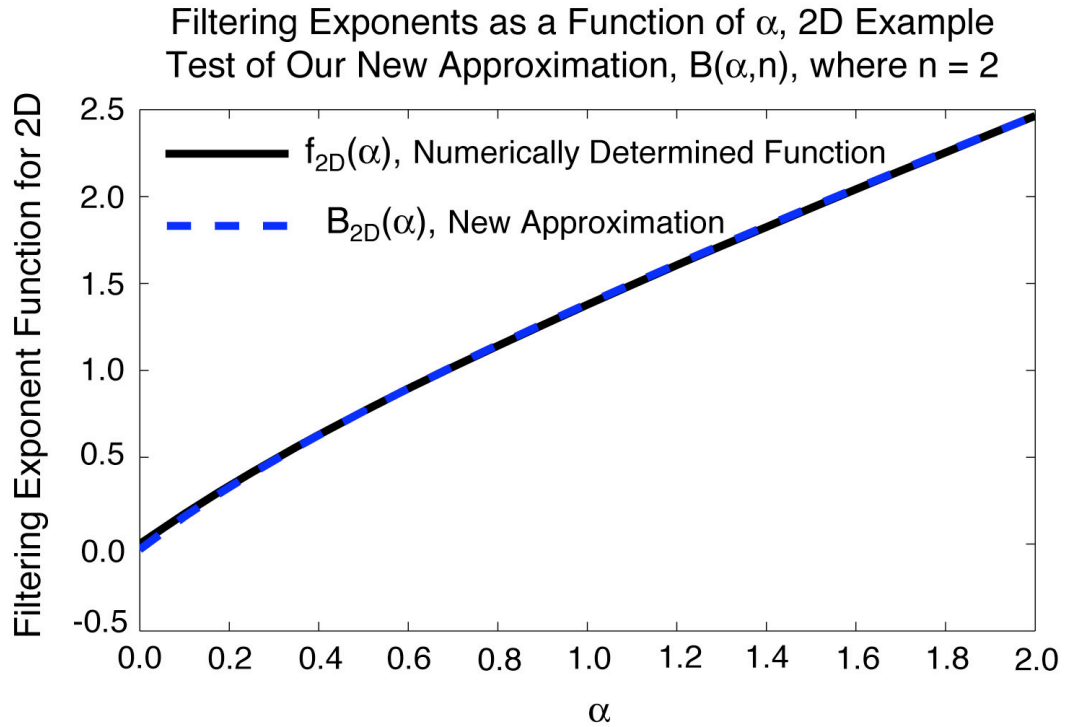


Figure 2.6. This is similar to Figure 2.5 except now our improved approximation, $B(\alpha, n)$ (dashed blue line), is plotted on top of the numerically determined curve, $f(\alpha, n)$ (solid black line). This time, our new approximation plots almost exactly on top of the numerically determined curve, $f(\alpha, n)$, indicating we have significantly improved our filtering exponent approximation. By visual inspection we choose hyperbolic functions to represent our new approximation. For 2D ($n = 2$) we have

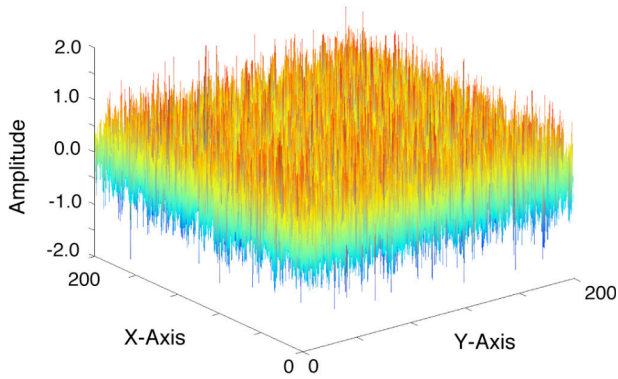
$$B(\alpha) = 2 \sqrt{\left[\left(\frac{\alpha + 2.5}{2.25} \right)^2 - 1 \right]} - 1$$

and for 3D ($n = 3$) it is

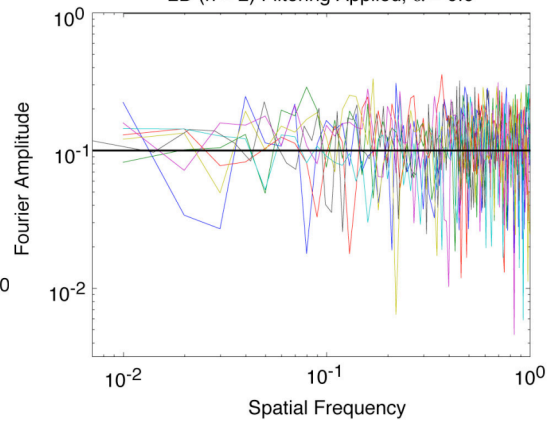
$$B(\alpha) = 4.5 \sqrt{\left[\left(\frac{\alpha + 7.5}{7.45} \right)^2 - 1 \right]} - 0.5.$$

These new approximations should be sufficient to produce our desired α smoothing for 1D cross sections.

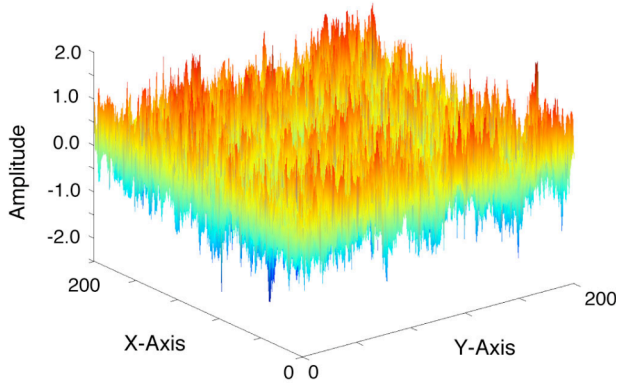
Smoothed Scalar Quantity with 2D Filter ($n = 2$), $\alpha = 0.0$



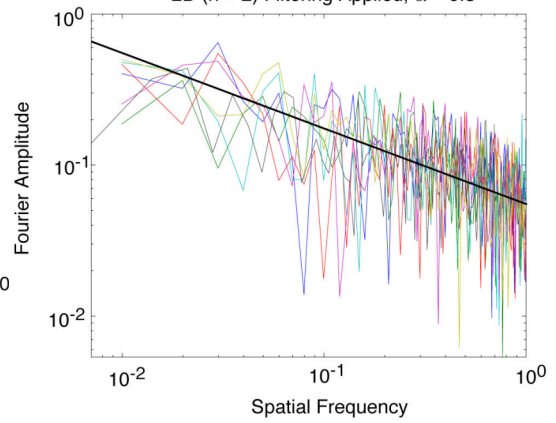
Fourier of Scalar Quantity Along 1D Cross Sections, 2D ($n = 2$) Filtering Applied, $\alpha = 0.0$



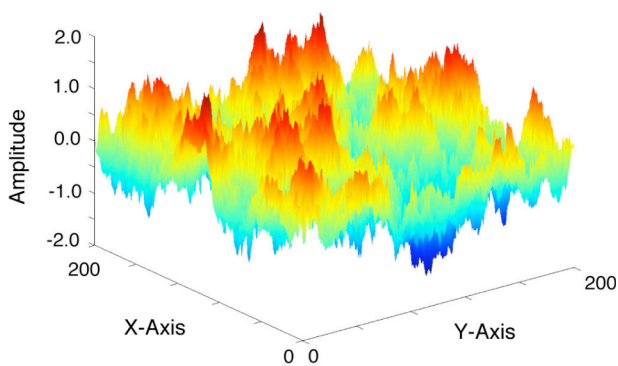
Smoothed Scalar Quantity with 2D Filter ($n = 2$), $\alpha = 0.5$



Fourier of Scalar Quantity Along 1D Cross Sections, 2D ($n = 2$) Filtering Applied, $\alpha = 0.5$



Smoothed Scalar Quantity with 2D Filter ($n = 2$), $\alpha = 1.0$



Fourier of Scalar Quantity Along 1D Cross Sections, 2D ($n = 2$) Filtering Applied, $\alpha = 1.0$

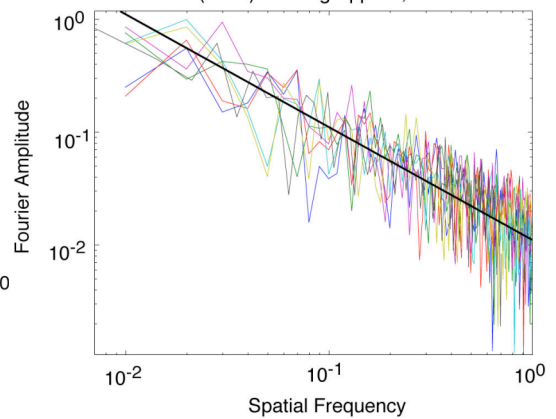
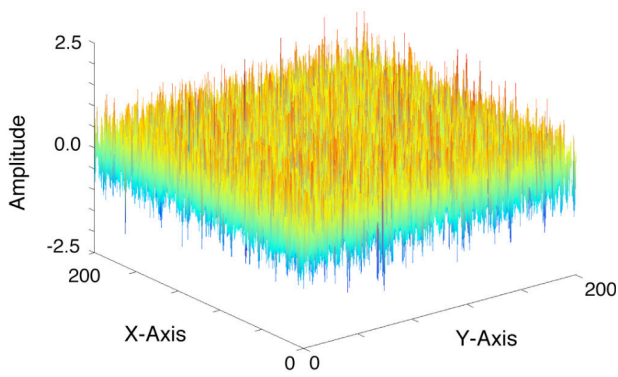


Figure 2.7. *Samples of our new smoothing approximation, $B(\alpha, n)$, for 2D ($n = 2$).*

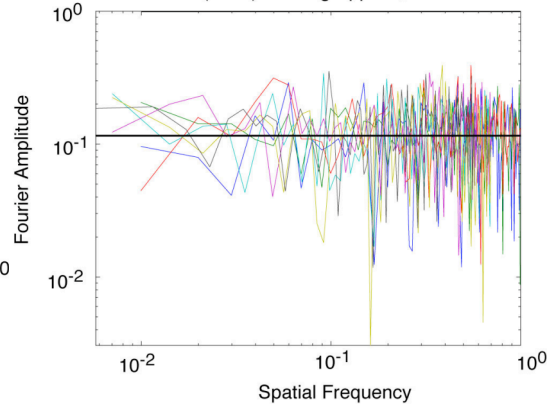
$\alpha = 0.0$ for the top row, $\alpha = 0.5$ for the middle row, and $\alpha = 1.0$ for the bottom row.

The left column is a 2D surface plot where the height and color indicate the amplitude of the scalar quantity. The right column shows a log-log Fourier amplitude spectra vs. spatial frequency for various 1D cross sections through the 2D grid where the solid black shows what the slope should be if our filter, $B(\alpha, n)$, is working properly. Note two features: 1) The slopes of the 1D cross sections are approximately correct. 2) As the filtering power, α , increases, the 2D spatial correlation of the values increases, i.e., it becomes spatially smoother as expected.

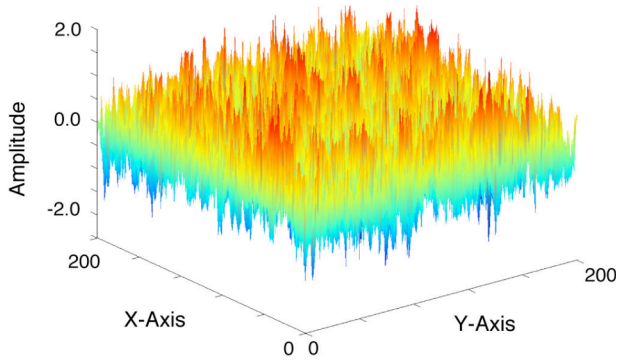
Smoothed Scalar Quantity with 3D Filter ($n = 3$), $\alpha = 0.0$



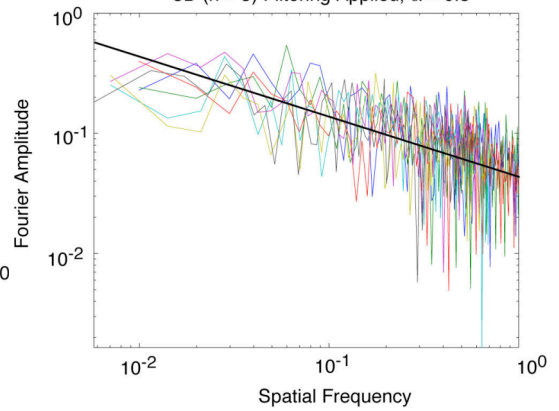
Fourier of Scalar Quantity Along 1D Cross-Sections, 3D ($n = 3$) Filtering Applied, $\alpha = 0.0$



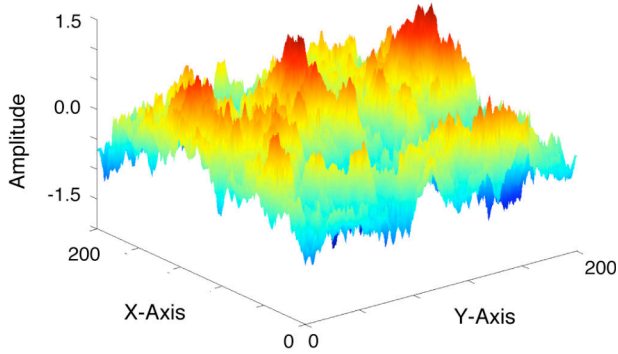
Smoothed Scalar Quantity with 3D Filter ($n = 3$), $\alpha = 0.5$



Fourier of Scalar Quantity Along 1D Cross-Sections, 3D ($n = 3$) Filtering Applied, $\alpha = 0.5$



Smoothed Scalar Quantity with 3D Filter ($n = 3$), $\alpha = 1.0$



Fourier of Scalar Quantity Along 1D Cross Sections, 3D ($n = 3$) Filtering Applied, $\alpha = 1.0$

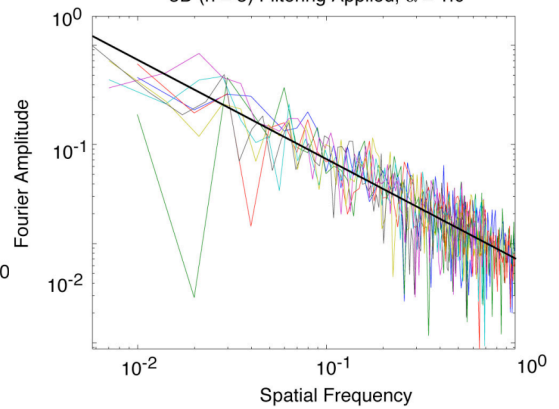


Figure 2.8. *This is very similar to Figure 2.7, except we have 2D cross sections through a 3D grid. It is meant to demonstrate our new 3D ($n = 3$) filtering approximation. In this case, the same seed data are used for the top ($\alpha = 0.0$), middle ($\alpha = 0.5$), and bottom ($\alpha = 1.0$) rows, to show what happens as α increases. Again 1D cross sections have approximately the proper spectral falloff, and as α increases, the observed spatial clumping in 2D and 3D increases.*

References

Barnsely, M., et al. (1988), *The Science of Fractal Images*, Springer-Verlag, New York.

Liu-Zeng, J., et al. (2005), The effect of slip variability on earthquake slip-length scaling, *Geophysical Journal International*, 162, 841–849.